Journal Name

ARTICLE

Facile Preparation of Robust Porous Photothermal Membrane with Antibacterial Ability for Efficient Solar-driven Interfacial Water Evaporation

Yaling Li, Xuexue Cui, Mingyu Zhao, Yunshi Xu, Leilei Chen, Zhijuan Cao, Shuguang Yang,* and Yi Wang*

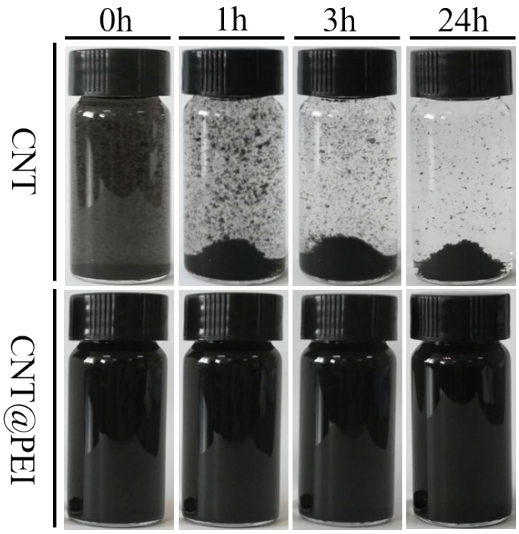

Fig. S1. Optical images of CNT and CNT@PEI aqueous solution after standing for different time periods.

Table S1. Zeta potentials of different membrane materials.

Samples	MCE	PEI	CNT	CNT@PEI
Zeta potential/mV	-33.8	27.8	-0.2	27.2

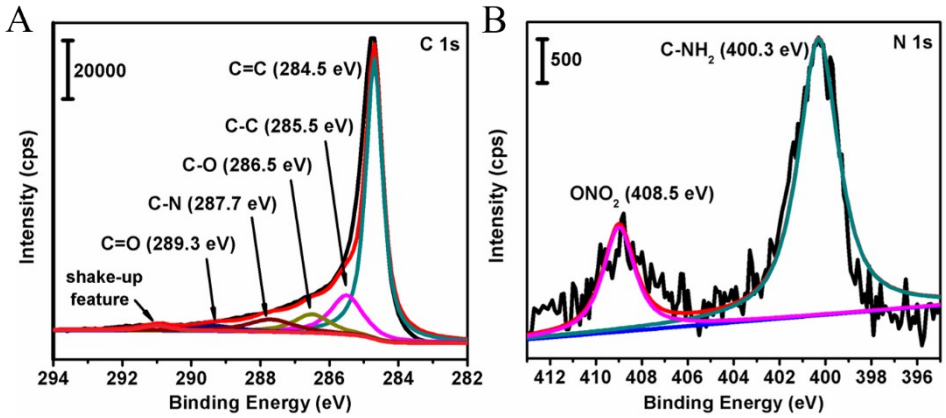

Fig. S2. Deconvoluted XPS spectra of C 1s (A) and N 1s (B) for CNT@PEI/MCE membrane.

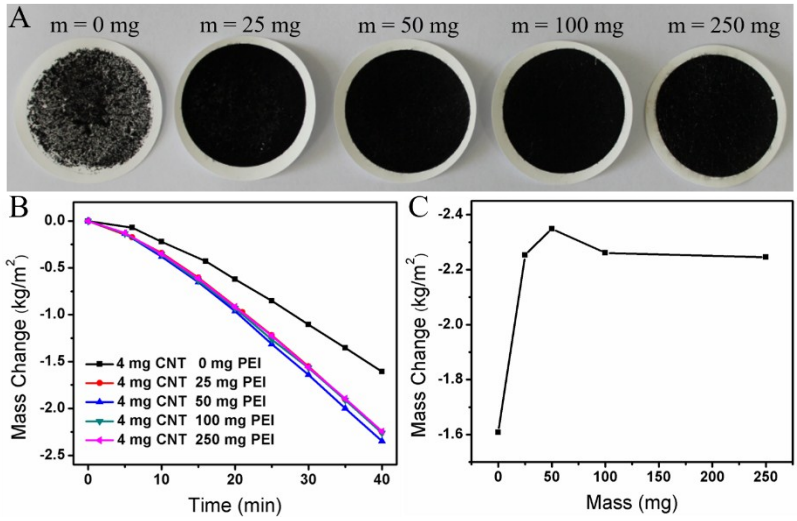

Fig. S3. (A) Optical images and (B, C) water evaporation performances under the simulated solar irradiation of CNT@PEI/MCE membranes with different amounts of PEI at a fixed amount of CNT.

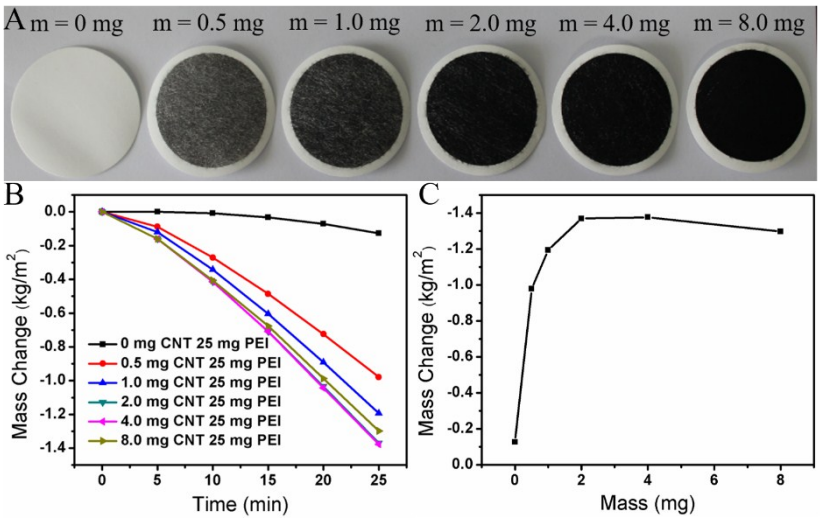

Fig. S4. (A) Optical images and (B, C) water evaporation performances under the simulated solar irradiation of CNT@PEI/MCE membranes with different amounts of CNT at a fixed amount of PEI.

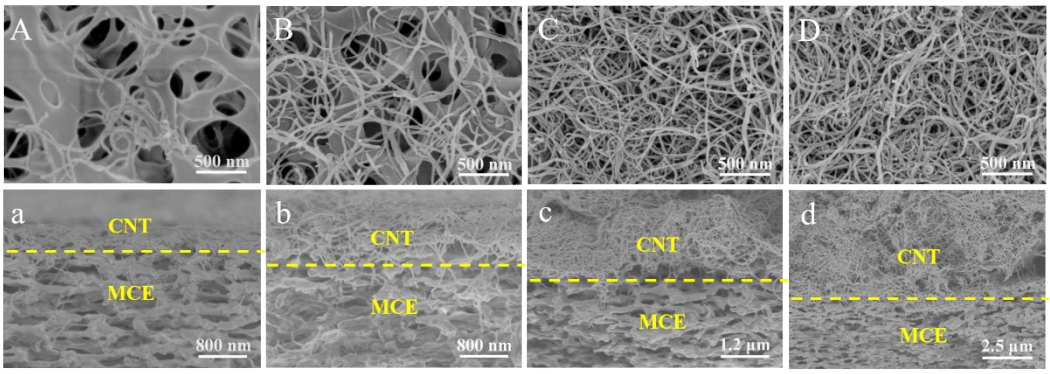

Fig. S5. Top-viewed (Up) and cross section-viewed (Bottom) SEM images of CNT@PEI/MCE membranes with different CNT layer thickness of M1 (A, a); M2 (B, b); M4 (C, c) and M5 (D, d).

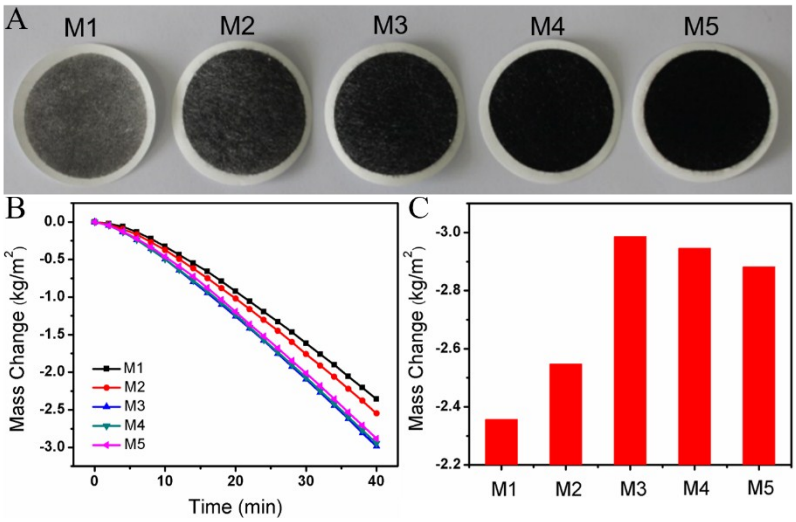

Fig. S6. (A) Optical images and (B, C) water evaporation performances under the simulated solar irradiation of CNT@PEI/MCE membranes with different CNT layer thickness.

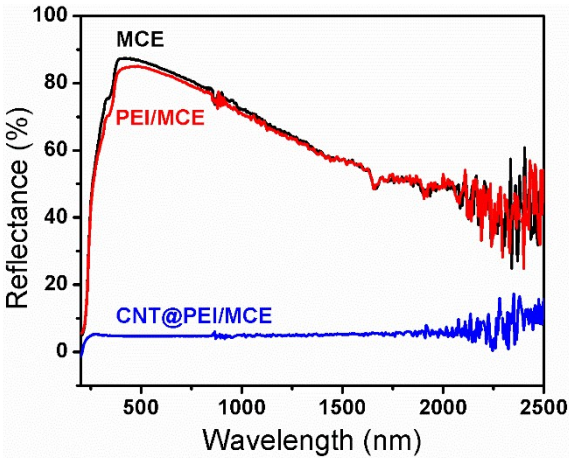

Fig. S7. Reflectance spectra of MCE, PEI/MCE and CNT@PEI/MCE.

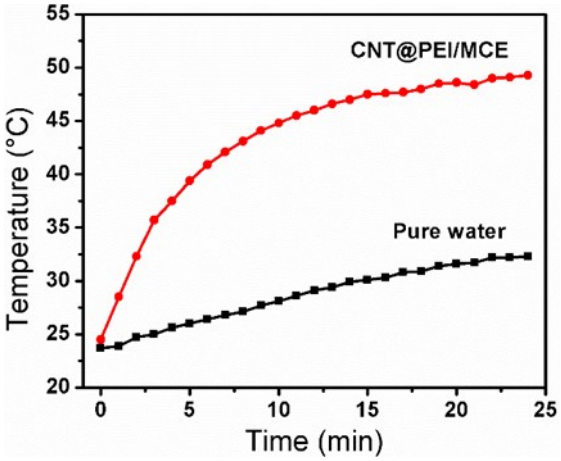

Fig. S8. The average interfacial temperature changes within the beaker aperture area of pure water and CNT@PEI/MCE system upon simulated solar illumination (5 kW m^{-2}).

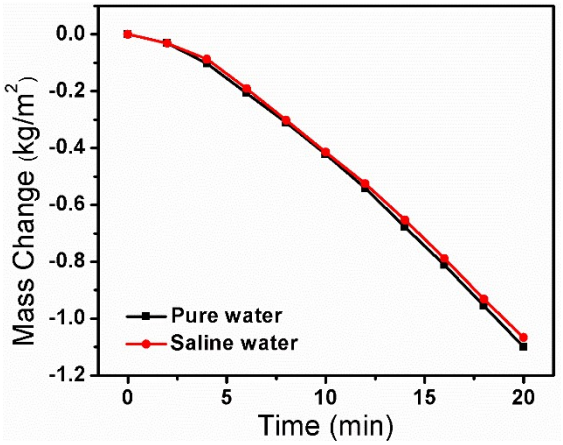

Fig. S9. Water evaporation rate curves of CNT@PEI/MCE floated on pure water and saline water via stimulated solar irradiation.

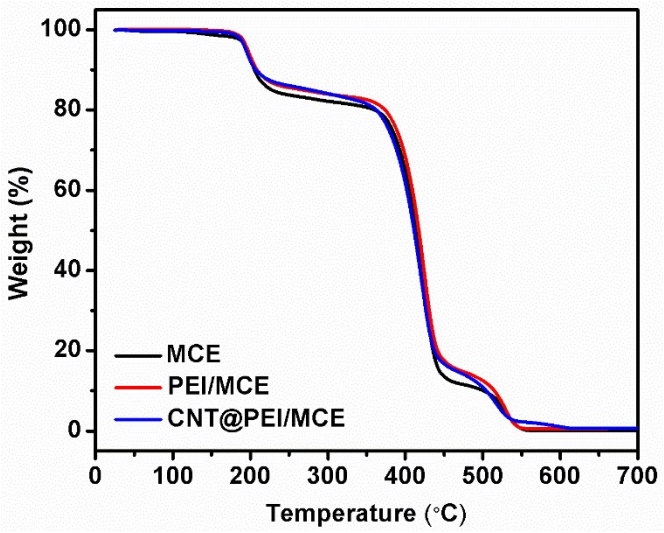

Fig. S10. TGA curves of MCE, PEI/MCE and CNT@PEI/MCE.

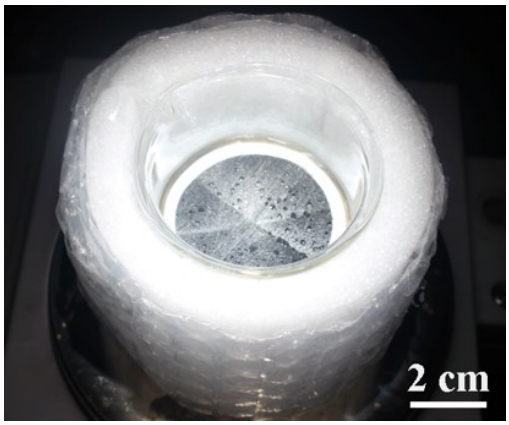

Fig. S11. Optical image of a folded CNT@PEI/MCE membrane with reserved water replenishment via the capillary pumping (some droplet on the surface).

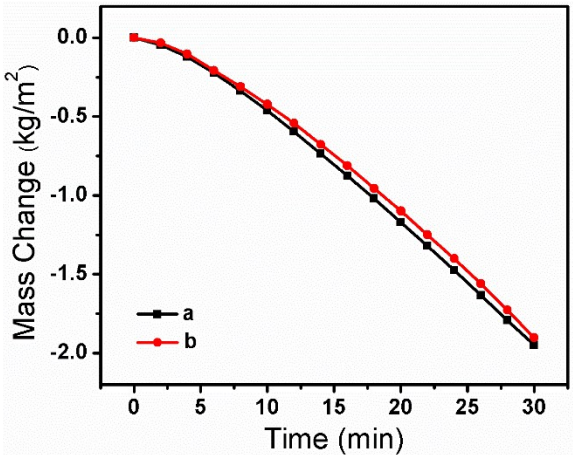

Fig. S12. Water evaporation rate curves of the CNT@PEI/MCE before (a) and after (b) 112 days storage.

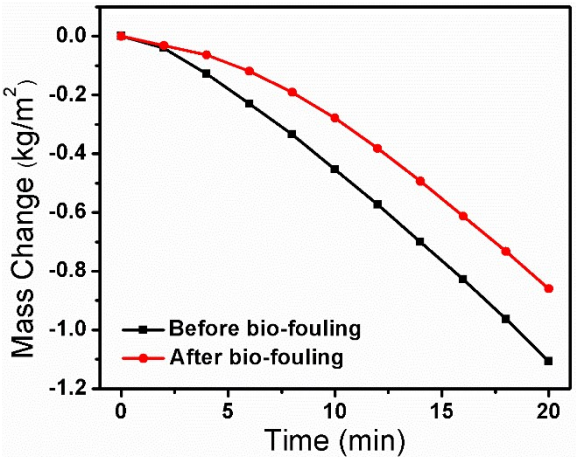

Fig. S13. Water evaporation performances under the simulated solar irradiation of CNT@PEI/MCE membranes before and after bio-fouling.

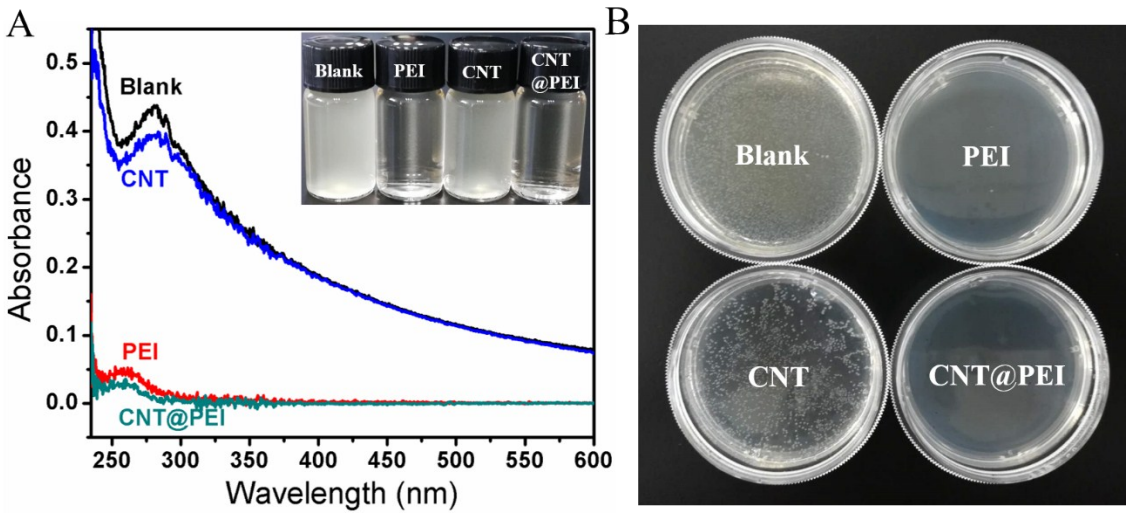

Fig. S14. (A) UV-vis absorption spectra and optical images (insets) of bacterial suspensions treated by blank, PEI, CNT and CNT@PEI, respectively. (B) Optical images of agar plates incubating with blank, PEI, CNT or CNT@PEI-treated bacterial suspensions.

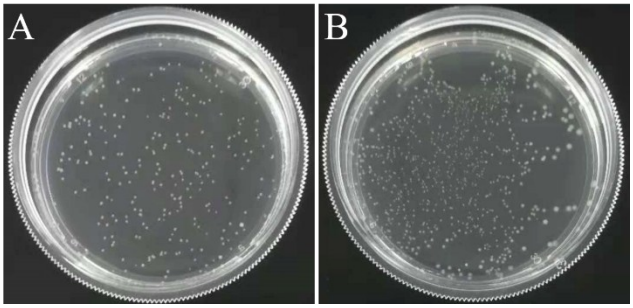

Fig. S15. Optical images of agar plates after incubating with the CNT@PEI/MCE before (A) and after eight cycles (B)-treated bacterial suspensions.